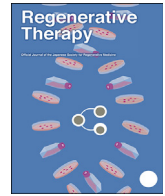




Contents lists available at ScienceDirect

Regenerative Therapy

journal homepage: <http://www.elsevier.com/locate/reth>

Original Article

Cisplatin induces differentiation in teratomas derived from pluripotent stem cells

Atsushi Kurata^{*}, Masakatsu Takanashi, Shin-ichiro Ohno, Koji Fujita, Masahiko Kuroda

Department of Molecular Pathology, Tokyo Medical University, 6-1-1, Shinjuku, Shinjuku-ku, Tokyo, Japan

ARTICLE INFO

Article history:

Received 12 March 2021
 Received in revised form
 30 April 2021
 Accepted 22 May 2021

Keywords:

Cisplatin
 Embryonic stem cells
 Induced pluripotent stem cells
 Immature teratoma
 Differentiation

ABSTRACT

Introduction: Currently, embryonic stem cells (ESCs) and induced pluripotent stem cells (iPSCs) can be induced to differentiate at the cellular level but not to form mature tissues or organs suitable for transplantation. ESCs/iPSCs form immature teratomas after injection into immunodeficient mice. In humans, immature teratomas often transform into fully differentiated mature teratomas after administration of anticancer agents.

Methods: We first investigated the ability of cisplatin to induce changes in mouse ESCs/iPSCs *in vitro*. Next, we designed experiments to analyze ESC/iPSC-derived immature teratoma tissue *in vivo* after treatment of cisplatin. Groups of six mice carrying ESC- or iPSC-derived teratomas were given either low or high dose intraperitoneal injection of cisplatin, while the control group received saline for 4 weeks. **Results:** Treatment of ESC/iPSC cultures with cisplatin for 3 days caused a dose-related decrease in cell numbers without inducing any morphological changes to the cells. ESC/iPSC-derived teratomas showed lower growth rates with a significantly higher mature components ratio in a concentration dependent manner after cisplatin treatment ($P < 0.05$); however, immunohistochemical analyses demonstrated a significantly reduced PCNA labelling index and an increase in an apoptosis marker on immature neural components ($P < 0.05$) along with emergence of h-Caldesmon⁺ mature smooth muscle cells in treated mice. Moreover, newly differentiated components not found in the control group, such as mature adipose tissue, cartilage, and pancreas, as well as striated muscle, salivary glands, gastric mucosa with fundic glands, and hair follicles emerged. The identities of these components were confirmed by immunostaining for specific markers.

Conclusions: Cisplatin has the ability to reduce immature components in ESC/iPSC-derived teratomas, presumably through apoptosis, and also to induce them to differentiate.

© 2021, The Japanese Society for Regenerative Medicine. Production and hosting by Elsevier B.V. This is an open access article under the CC BY-NC-ND license (<http://creativecommons.org/licenses/by-nc-nd/4.0/>).

Abbreviations: ALP, alkaline phosphatase; α -SMA, α -smooth muscle actin; ATP4B, ATPase H⁺/K⁺ transporting beta subunit; CR, chemotherapeutic retroconversion; DMEM, Dulbecco's modified Eagle's medium; ESC, embryonic stem cell; FCS, fetal calf serum; HE, hematoxylin and eosin; iPSC, induced pluripotent stem cell; KSR, knockout serum replacement; LIF, leukemia inhibitory factor; MEF, mouse embryonic fibroblast; PBS, phosphate buffered saline; PCNA, proliferating cell nuclear antigen; RAG, recombination activating gene; RLU, relative light units; RT, room temperature; ssDNA, single stranded DNA.

^{*} Corresponding author. Department of Molecular Pathology, Tokyo Medical University, 6-1-1, Shinjuku, Shinjuku-ku, Tokyo, 160-8402, Japan. Fax: +81 3 3351-6173.

E-mail address: akurata@tokyo-med.ac.jp (A. Kurata).

Peer review under responsibility of the Japanese Society for Regenerative Medicine.

<https://doi.org/10.1016/j.reth.2021.05.005>

2352-3204/© 2021, The Japanese Society for Regenerative Medicine. Production and hosting by Elsevier B.V. This is an open access article under the CC BY-NC-ND license (<http://creativecommons.org/licenses/by-nc-nd/4.0/>).

1. Introduction

Tissue regeneration requires the delivery of specific cell types or cell products to support or replace degenerated or damaged organs. Pluripotent stem cells, such as embryonic stem cells (ESCs) and induced pluripotent stem cells (iPSCs), have the potential to be used as the source of such cells and cell products [1]. However, at present, pluripotent stem cells can only be induced to differentiate at the cellular level and differentiation into tissues or organs has yet to be achieved [2].

When injected into immunodeficient mice, pluripotent stem cells form teratomas with differentiation of three germ cell layers; as these teratomas are immature and potentially malignant, they are inappropriate for use in therapeutic transplantation [3]. In recent years, there have been attempts to differentiate engraftable

blood stem cells and muscle primordia from pluripotent stem cell-derived teratomas [4,5]; to date, no clearly differentiated tissues have been produced.

In humans, spontaneous teratomas arise predominantly in ovaries: 99% are benign mature teratomas, and the remaining 1% are malignant immature teratomas similar to those derived from pluripotent stem cells [6]. Histological analyses of immature teratomas show that they consist of not only mature but also immature components, the latter containing most commonly immature neural tissues. Immature teratomas are classified into grades 1 to 3 based on the relative amounts of immature neural tissue. In human patients, anticancer drugs are generally administered after surgery except for grade 1 teratomas limited to ovaries [7].

Human ovarian immature teratomas often transform into fully differentiated mature teratomas when disseminated or metastatic foci are resected after administration of an anticancer therapy (typically containing cisplatin); this phenomenon is called chemotherapeutic retroconversion (CR) [8]. Although the frequency of CR is uncertain, a literature review found that mature teratomas or mature glial implants were present in 20 of 48 (42%) second-look laparotomies after chemotherapy for malignant ovarian germ cell tumors [9]. With regard to the etiology of CR, at least 2 mechanisms have been proposed: (1) chemotherapy promotes the conversion of immature tissues into mature tissues; (2) chemotherapy selectively destroys immature components allowing mature tissue to flourish. Currently, most of the available evidence favors the second possibility [10,11]; however, we previously pointed out that the first mechanism could be used to explain consecutively resected metastatic foci during chemotherapy in a patient with an ovarian immature teratoma [12].

The present study was designed to assess changes in ESCs and iPSCs *in vitro* after treatment with cisplatin, and to analyze immature teratoma tissues derived from ESCs and iPSCs *in vivo* after treating tumor-bearing immunodeficient mice with intraperitoneal injection of cisplatin. The aim of the study was to elucidate the etiology of CR with a view to the long-term goal of applying it to regenerative medicine.

2. Materials and methods

2.1. Derivation and culture of mouse ESCs

The EGR-G101 ES cell line was previously established from C57BL/6-Tg (CAG/Acr-EGFP) C3–N01-FJ002Osb [13]. The cells were cultured in knockout serum replacement (KSR) medium, which consisted of high-glucose Dulbecco's modified Eagle's medium (DMEM; Gibco, Frederick, MD, USA) supplemented with 15% KSR (Gibco), 2 mM glutamine (Gibco), 1 mM sodium pyruvate (Gibco), 0.1 mM non-essential amino acids (Gibco), 0.1 mM 2-mercaptoethanol (Gibco), and 1000 U/ml leukemia inhibitory factor (LIF; Merck Millipore, Darmstadt, Germany), on a mitomycin-inactivated mouse embryonic fibroblast (MEF) feeder layer in 0.1% gelatin-coated 10 cm culture plates. ESC colonies were mechanically passaged every 3 days into clumps, with a split ratio of 1:3, on MEF feeder cells.

2.2. Culture of mouse iPSCs

iPSCs (iPS-MEF-Ng-440A3) were purchased from RIKEN Cell Bank (Ibaraki, Japan). The cells were cultured in DMEM containing 15% fetal calf serum (FCS; Gibco), 2 mM glutamine, 1 mM sodium pyruvate, 0.1 mM non-essential amino acids, 0.1 mM 2-mercaptoethanol, and 1000 U/ml LIF on a mitomycin-inactivated MEF feeder layer in 0.1% gelatin-coated 10 cm dishes. iPSC

colonies were mechanically passaged every 3 days into clumps, with a split ratio of 1:3, on MEF feeder cells.

2.3. Cisplatin treatment of mouse ESCs and iPSCs

ESCs and iPSCs were seeded onto 12 well plates with 0.1% gelatin-coated mitomycin-inactivated MEF at 1×10^5 cells/1 ml/well. Cisplatin (0.5 mg/ml) (Maruko: Yakult, Tokyo, Japan) was serially diluted twofold from 20- to 20,480-fold (cisplatin concentrations from 25 to 0.0244 μ g/ml) with phosphate buffered saline (PBS, pH 7.4) and 20 μ l were added daily for 3 days starting on the next day after seeding. Negative controls received PBS. On the day following the third addition, the cells were imaged and alkaline phosphatase (ALP) activity was detected by a cytochemical assay using a Leukocyte ALP Kit (#ALP-TK1; Sigma–Aldrich Japan, Tokyo, Japan) according to the manufacturer's protocol. A cell proliferation assay was also performed.

2.4. Cell proliferation assay

The effect of cisplatin on the numbers of ESCs and iPSCs was evaluated using a CellTiter-Glo 2.0 Assay (Promega, Madison, WI, USA) according to the manufacturer's instructions. The luminescent signal was measured using Infinite F200 Pro (TECAN, Kanagawa, Japan). Luminescence was measured as relative light units (RLU) and the mean \pm SD of triplicate wells was obtained.

2.5. Transplantation of ESCs and iPSCs into immunodeficient mice

When ESCs/iPSCs reached 70–80% confluence (cultured as described above), they were trypsinized, washed with PBS, resuspended in 1 ml PBS, and injected subcutaneously (6×10^6 ESCs/iPSCs in a total volume of 100 μ l) into the back and left femur of three 10-week-old recombination activating gene 2 (RAG2) $-/-$ mice (Sankyo Labo Service, Tokyo, Japan) in each experiment. The mice were housed in cages (up to 5 animals per cage) and provided *ad libitum* access to water and food (FR-1; Funabashi Farm, Chiba, Japan). The animal rooms were maintained as a temperature-controlled (21–25 °C) and light-controlled (12L:12D cycle, lights on at 0800 h) environment. The mice were bred and maintained under specific pathogen-free conditions. All animal care and procedures performed in this study were approved by the Animal Research Committee of Tokyo Medical University, and conformed to its guidelines for animal experiments. Five weeks after the injection, subcutaneous tumors up to 20 mm in the longest diameter were detected. The mice were then sacrificed; the tumors were dissected and $3 \times 3 \times 3$ mm pieces of the tumors were passaged subcutaneously into six other mice. Six weeks later, subcutaneous tumors were again recovered and $3 \times 3 \times 3$ mm pieces were transplanted subcutaneously into fresh mice; in total, 10 mice in 3 groups for both ESC-derived and iPSC-derived tumor experiments were obtained. In order to unify gender for each experiment, we used female mice for the ESC transplantations and male mice for the iPSC transplantations.

2.6. Cisplatin injections into mice bearing tumors derived from ESCs and iPSCs

When all the inoculated subcutaneous tumors became palpable 10 days after successive subcutaneous transplantation of tumors, tumor-bearing mice were given weekly intraperitoneal injections of cisplatin (Maruko) at either a low or high dose (2.5 or 5 mg/kg/week, respectively). Mice in the control group received saline. Because two tumors in control group reached 20 mm in the longest diameter after 3 weeks, two mice with the biggest tumors in each

group were sacrificed and exclude from the experiments. After 4 weeks, tumor-bearing mice were sacrificed except for two mice with the smallest tumors in each group; these two mice were given weekly intraperitoneal injections of cisplatin and sacrificed after a further 4 weeks. The tumors were removed and then fixed in 10% formalin overnight at room temperature (RT), and then embedded in paraffin. Staining of histological sections was performed with hematoxylin and eosin (HE).

2.7. Histological evaluation and statistical analyses

Light microscopical analyses were performed using a Carl Zeiss HAL 100 microscope with a W-PI $10\times/23$ ocular lens. The extent of necrosis in each tumor was first evaluated. With the exception of the center of large tumors where massive necrosis was present, ten randomly chosen fields of view ($100\times$ magnification) were evaluated for the presence of a necrotic area; absence of necrosis was graded as 0, presence of necrosis as 1. A “necrosis score” of 0–10 (11-tier scoring) was then established based on the sum of the evaluations in the 10 fields of view. Subsequently, another ten fields of view ($100\times$ magnification) without necrosis were selected in each tumor, and analyzed to determine whether immature or mature components were dominant for each field of view; dominance of immature components was graded as 0, dominance of mature components as 1. A “maturation score” from 0 to 10 was likewise established. Tukey–Kramer tests were used to identify significant differences in the necrosis score and maturation score between the three groups. These scores were also subjected to a Spearman's rank correlation analysis. These statistical analyses were performed using excel statistics for Macintosh ver3.0 (Esumi, Tokyo, Japan), and the level of significance was set at $P < 0.05$. Detailed histological evaluations were also carried out to determine the types of tissue that differentiated in each tumor. With regard to assessment of mature tissue, care was taken to exclude the possibility of host derivation such as mature adipose tissue intruding from the tumor margin.

2.8. Immunohistochemistry of selected tissues

For both ESC-derived and iPSC-derived teratomas, six samples from the 4-week high dose cisplatin group and 6 samples from the 4-week controls were selected for immunostaining, *i.e.*, a total of 24 samples were selected. In addition, eight samples from the 8-week high dose cisplatin group and a control were selected and used for immunostaining of α -smooth muscle actin (α -SMA) and h-Caldesmon.

From paraffin embedded selected samples, 4 μm -thick sections were cut, and immunostaining was then performed. The standard polymer method was used for immunohistochemical staining using antibodies to proliferating cell nuclear antigen (PCNA, mouse, clone PC10, 1:2000 dilution, Dako), single stranded DNA (ssDNA, rabbit, polyclonal, 1:1000 dilution, Dako), α -SMA (mouse, clone 1A4, 1:100 dilution, Dako, Glostrup, Denmark), h-Caldesmon (mouse, clone h-CD, 1:100 dilution, Dako), ATPase H⁺/K⁺ transporting beta subunit (ATP4B, mouse, clone 2G11, 1:2000 dilution, Thermo Fisher Scientific, Waltham, MA, USA), aquaporin 5 (rabbit, polyclonal, 1:500 dilution, abcam, Cambridge, UK), and carboxypeptidase A2 (rabbit, clone CPA2, 1:500 dilution, Sino Biological, Beijing, China). Deparaffinized and hydrated sections were treated with 0.3% hydrogen peroxide in methanol for 15 min to block endogenous peroxidase activity. Sections for immunostaining of PCNA were autoclaved in 1 mmol/L Tris–EDTA buffer (pH 9.0), while those for h-Caldesmon, carboxypeptidase A2, and ATP4B were autoclaved in 10 mmol/L sodium citrate buffer (pH 6.0), at 121 °C for 10 min to expose antigens, and then cooled for 30 min. After rinsing in 0.01 mol/L PBS,

sections were incubated in blocking milk buffer (1% dry skimmed milk in PBS) for 10 min and incubated with affinity-purified primary antibodies for 90 min at RT. Thereafter, they were incubated with Envision™ + Dual Link peroxidase (Dako) at RT for 30 min. The peroxidase reaction was visualized using 0.02% 3,3'-diaminobenzidine tetrahydrochloride and 0.01% hydrogen peroxide in 0.1 mol/L PBS. Finally, nuclear counterstaining was performed with Mayer's hematoxylin.

2.9. Evaluation of immunostained sections and statistical analyses

All immunostained sections were evaluated in detail. In particular, the identities of immunopositive tissues after ATP4B, aquaporin 5, and carboxypeptidase A2 staining were confirmed by screening serial HE stained sections. The presence or absence of h-Caldesmon⁺ mature smooth muscle cells between cisplatin-treated and non-treated groups was statistically compared by a Chi-square test. After α -SMA and h-Caldesmon staining, blood vessels were evaluated for indications of positive staining. After PCNA and ssDNA staining, images of the sections were captured using a whole-slide scanner (Nanozoomer, Hamamatsu Photonics, Hamamatsu City, Japan), and examined using the associated proprietary viewing software. Three 0.13×0.13 mm squares (total area 0.169 mm^2) were randomly chosen from immature neural components in the same field for analysis of PCNA and ssDNA. The number of positive nuclei per square was determined for each specimen. Inflammatory cells infiltrating the tumor served as an internal positive control. The mean proportions of PCNA⁺ to ssDNA⁺ nuclei in cisplatin-treated and non-treated groups were statistically compared using Student's t-test.

3. Results

3.1. In vitro cisplatin treatment of mouse ESCs/iPSCs and cell proliferation assay

ESCs and iPSCs were seeded onto 12-well plates and treated with 20 μl of a serially diluted cisplatin solution (cisplatin concentrations from 0.0244 to 25 $\mu\text{g}/\text{ml}$) for 3 days. Cell proliferation assays performed after treatment revealed that the numbers of ESCs and iPSCs decreased with increasing cisplatin concentrations compared with PBS-treated controls (Fig. 1a and b, $P < 0.01$). The decreased number of cells was paralleled by a decrease in colony-forming ability verified by ALP activity; however, no morphological changes were observed in the cells (Fig. 1c–h).

3.2. Comparison of teratomas after cisplatin treatment

It was evident that the cisplatin treatment for 4 weeks caused lower growth rates of the ESC- and iPSC-derived tumors in a dose dependent manner as shown by decrease in their volumes (Fig. 2a). The mean necrosis score and maturation score of the tumors in each group was compared. A Tukey–Kramer test showed that a significantly decreased necrosis score was found for the high dose group compared with the control (Fig. 2b and c, $P < 0.05$). Conversely, the cisplatin treatment caused a significant increase in the maturation score in a dose dependent manner (Fig. 2d and e, $P < 0.01$) as visualized in representative HE stained sections (Fig. 2f and g). Spearman's rank correlation analysis also revealed that the necrosis score was inversely correlated with the maturation score ($P < 0.05$) in both ESC- and iPSC-derived tumors in total ($n = 18$) in mice treated for 4 weeks.

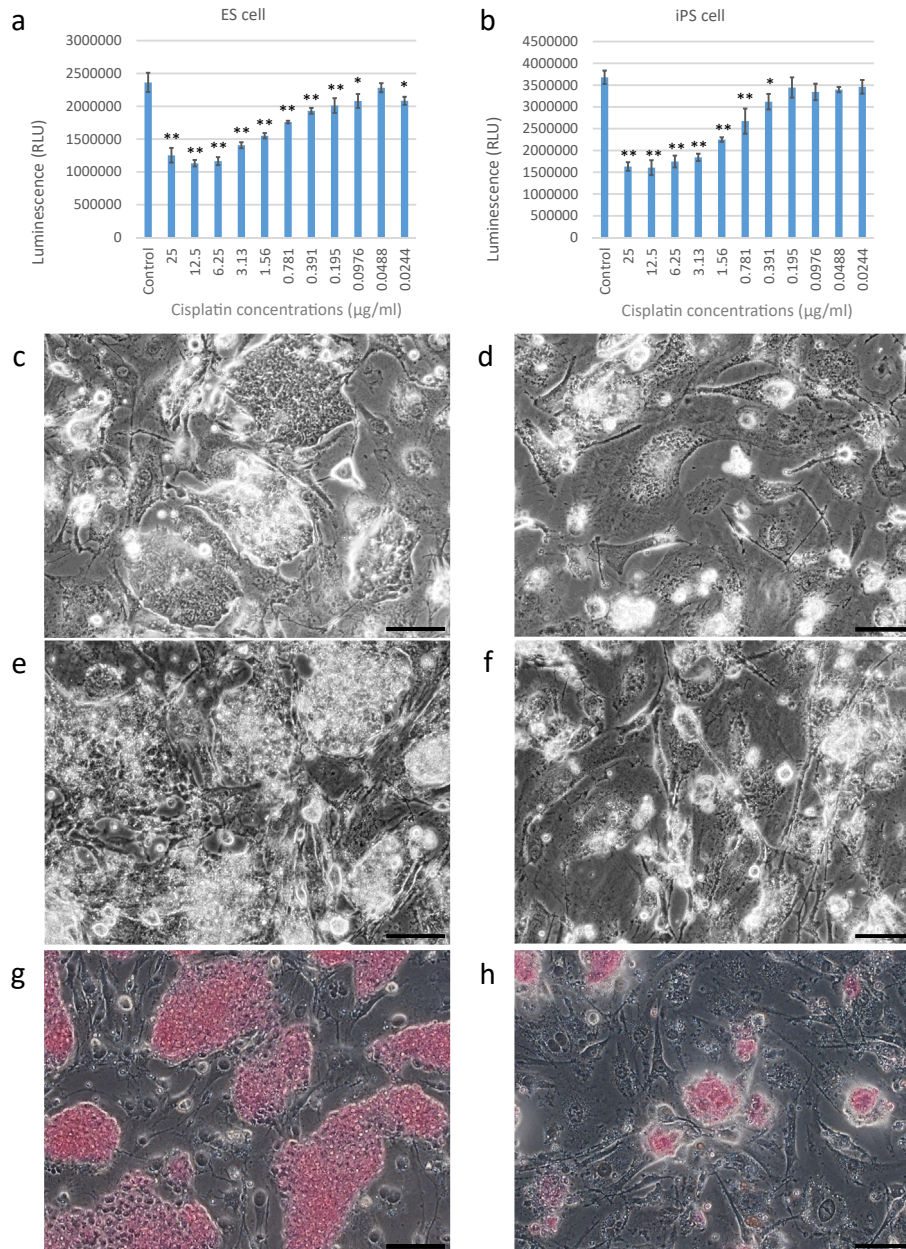


Fig. 1. ESCs/iPSCs *in vitro* after treatment with cisplatin. Cell proliferation assays for ESCs (a) and iPSCs (b) (vertical axis: Luminescence (Relative Luciferase Unit: RLU)) show a dose-related decrease (horizontal axis: cisplatin concentrations from 25 to 0.0244 μg/ml) compared with negative control treated with PBS, after treatment with 20 μl/day for 3 days. Compared with the negative control (c, e, g), cells given a high-dose cisplatin treatment showed decreased colony-forming ability (d, f, h) verified by alkaline phosphatase (ALP) activity (g, h); however, no changes to cell morphology were observed (c, d: ESCs; e–h: iPSCs; c–g: × 200; scale bar: 100 μm). *P < 0.05 and **P < 0.01 by Tukey–Kramer test in comparison with controls.

3.3. Comparison of markers for proliferation and apoptosis along with emergence of mature smooth muscle cells in teratomas

Immature neural components are commonly observed in teratomas regardless of their state of maturation; a decrease in immature neural components is a marker of maturity. Immunostaining for PCNA showed that immature neural components in teratomas of the high dose cisplatin treated mice had a lower mean PCNA labelling index compared with controls that received saline (Fig. 3a and b); this reduction was statistically significant by Student's t-test (Fig. 3c and d, $P < 0.05$). By contrast, the ssDNA labelling index increased significantly in the high dose treatment

group compared with controls in both ESC- and iPSC-derived tumors (Fig. 3e–h; $P < 0.05$). h-Caldesmon⁺ mature smooth muscle cells were never observed in the controls but were found in the 4-week high dose treatment groups: they were present in 4 of 6 ESC-derived tumors and 5 of 6 iPSC-derived tumors (Fig. 3i); the differences between the controls and treated groups were statistically significant (Chi-square tests, $P < 0.05$) in both ESC- and iPSC-derived tumors. Smooth muscle cells in the walls of vessels were immunopositive for α-SMA regardless of cisplatin treatment. Although vessels with h-Caldesmon⁺ smooth muscle cells were not observed after cisplatin treatment in the 4-week groups, they did appear sporadically in all 4 specimens at 8 weeks after cisplatin

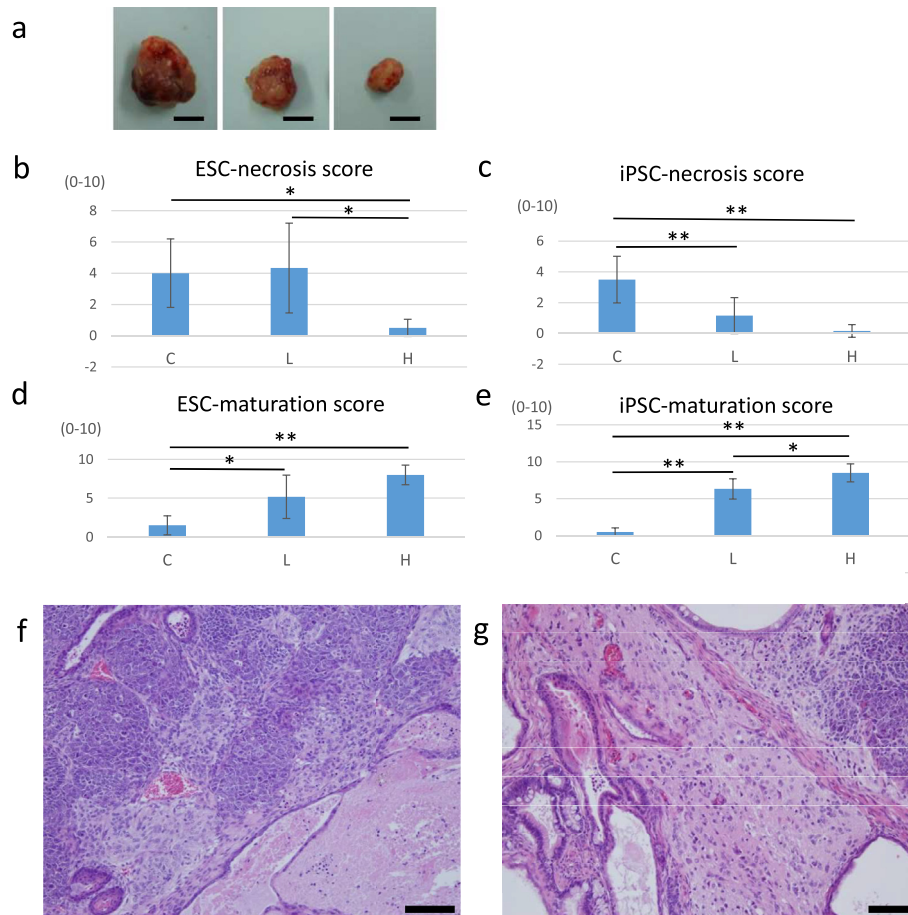


Fig. 2. Comparison of ESC/iPSC-derived teratomas with or without cisplatin treatment. (a) Representative tumors from control mice that received a saline injection (left) compared to low (center) and high (right) dose cisplatin treatments for 4 weeks (scale bar: 1 cm). Mean necrosis score (b, c), and maturation score (d, e) in control mice (bar C in each group) and mice that received low (bar L) or high (bar H) doses of cisplatin. Standard deviations are shown. (b, d) Tumors derived from ESCs. (c, e) Tumors derived from iPSCs. Cisplatin treatment of ESC/iPSC-derived tumors decreased tumor volumes, and caused a significant reduction in the necrosis score and increase in the maturation score in a dose dependent manner. * $P < 0.05$ and ** $P < 0.01$ by Tukey–Kramer test. (f) Representative non-treated tumor shows a predominance of immature neural elements (upper left) and necrosis (lower right). (g) Representative tumor from the high dose treatment shows a predominance of mature neural elements (center) (f, g; HE staining, $\times 100$; scale bar: 100 μm).

treatment (Fig. 3j). No h-Caldesmon⁺ cells were present in tumors from control mice at 4 or 8 weeks.

3.4. Detailed histological evaluation of teratomas after cisplatin injection

Detailed histological evaluation by HE staining of tumors derived from ESCs/iPSCs after 4- and 8-week treatment along with controls demonstrated that columnar epithelium, squamous epithelium, mature and immature neural elements, and fibrous tissue were present in all specimens. In addition to these tissues, immature cartilage appeared in most specimens of most groups. Immature pancreas, bone, and lipoblasts were also identified, albeit infrequently.

Only specimens from cisplatin treated mice contained mature tissues such as mature adipose tissue, cartilage with lacunae, striated muscle, salivary glands accompanied by mucinous glands, gastric mucosa with fundic glands, pancreas with the presence of polarity and centroacinar cells, and hair follicles (Fig. 4). All of these components were found relatively infrequently and were present in small, scattered amounts. The various tissues identified in the tumors from control and treated mice (with the exception of the ubiquitous components listed above) are described in Table 1.

3.5. Immunohistochemical evaluation of specific tissues in teratomas

Various tissues were obtained from control and cisplatin treated mice and analyzed immunohistochemically for the presence of different proteins (Fig. 5). Fundic glands in the gastric mucosa, mature salivary glands, and mature pancreas showed positive staining for ATP4B, aquaporin 5, and carboxypeptidase A2, respectively, in tissue sections from cisplatin-treated mice; these three antibodies did not give positive staining in the control group, with the exception of the immature pancreas that showed immunostaining by carboxypeptidase A2.

4. Discussion

Here, we investigated the cause of CR by *in vitro* treatment of ESCs/iPSCs with cisplatin and also by *in vivo* examination of the effects of cisplatin on ESC/iPSC-derived teratomas; to the best of our knowledge, this is the first such investigation on teratomas. The addition of cisplatin to ESC/iPSC cultures decreased cell numbers in a concentration dependent manner. The *in vivo* treatment of mice with ESC/iPSC-derived teratomas resulted in lower growth rates and an increase in the proportion of maturation components in the tumors. Additionally, differentiated components appeared that

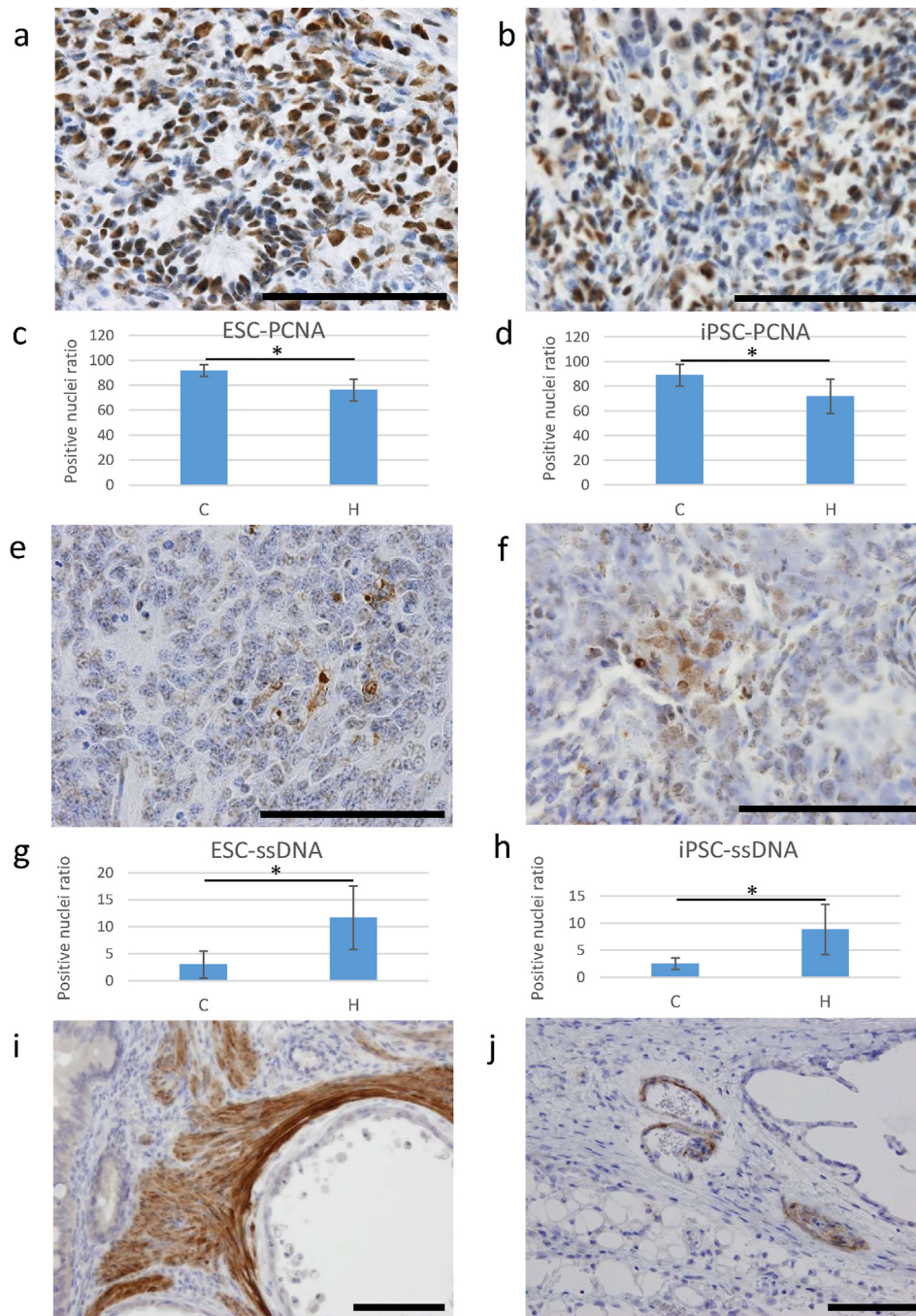


Fig. 3. Immunohistochemistry for PCNA, ssDNA, and h-Caldesmon. Photomicrographs of teratomas derived from ESCs/iPSCs after intraperitoneal treatment with high dose cisplatin along with controls that received saline, and comparison of the positive signal ratio after 4-week high dose treatment (bar H) with controls (bar C). (a) In controls, 90% PCNA⁺ nuclei were observed. (b) PCNA⁺ nuclei decreased to 70% in the high dose treatment group (× 400, scale bar: 100 μm). (c, d) Decreased mean PCNA labelling index in the high dose treatment group compared with controls. (e) 1% ssDNA⁺ nuclei were observed in the controls. (f) ssDNA⁺ nuclei increased to 20% in the high dose treatment group (× 400, scale bar: 100 μm). (g, h) Increased mean ssDNA labelling index in the high dose treatment group compared with controls. (i, j) Immunostaining of h-Caldesmon. Positively stained mature smooth muscle cells (i) and vascular wall (j) (i, j: × 200, scale bar: 100 μm).

were not found in the non-treated control group. Our findings indicate that cisplatin has the ability not only to reduce the immature components of ESC/iPSC-derived teratomas but also to induce differentiation within the tumors. We propose that both of these abilities underlie the phenomenon of CR.

Our finding that cisplatin treatment of mouse ESCs/iPSCs *in vitro* resulted in dose-related cell death and decreased colony-

forming ability (paralleled by decreased ALP activity, which is a marker for ESC/iPSC colonies [14]) is consistent with a previous report on ESCs [15]. Similar results have also been reported for human and mouse embryonal carcinoma cell lines [11], which share many characteristics with ESCs [16]. These findings are consistent with the ability of cisplatin to bind to DNA and selectively kill rapidly dividing cells [17]. Further, we did not identify

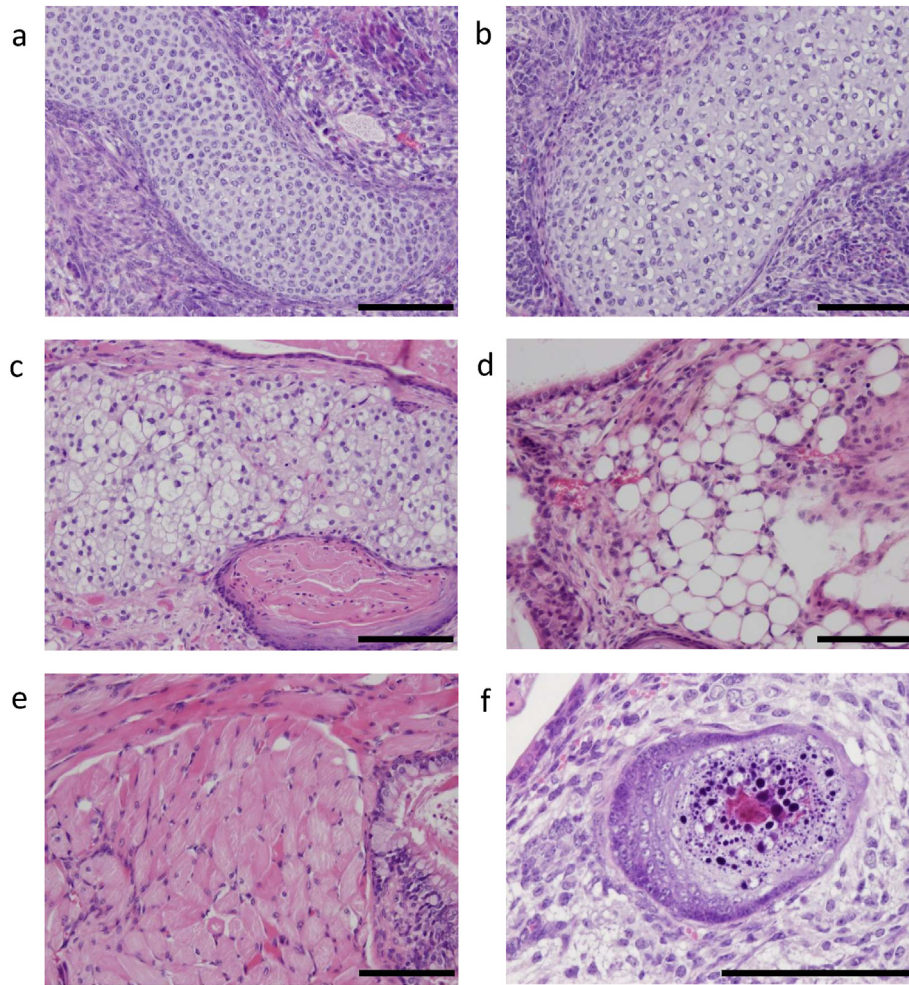


Fig. 4. Photomicrographs (HE staining) of teratomas derived from ESCs/iPSCs with (b, d–f) or without (a, c) intraperitoneal injection of cisplatin. (a) Immature cartilage without lacunae (× 200). (b) Mature cartilage with lacunae (× 200). (c) Lipoblasts with fine lipid droplets (× 200). (d) Mature fat tissue with large lipid droplets (× 200). (e) Muscles with striation (× 200). (f) Hair follicle (× 400). (scale bar: 100 μm).

Table 1

Immature and mature tissues other than columnar and squamous epithelium, neural elements, and fibrous tissue in teratomas of different treatment groups.

Cisplatin treatment	ESC-derived teratomas		iPSC-derived teratomas	
	Immature tissue	Mature tissue	Immature tissue	Mature tissue
4 w non-treated (n = 6)	Cartilage (n = 5), lipoblasts (n = 1), pancreas (n = 1)		Cartilage (n = 5), lipoblasts (n = 3), pancreas (n = 2), bone (n = 1)	
4 w low dose (n = 6)	Cartilage (n = 4), lipoblasts (n = 1), pancreas (n = 1), bone (n = 1)	Cartilage (n = 2), fat (n = 2), striated muscle (n = 1), hair follicle (n = 1)	Cartilage (n = 3), lipoblasts (n = 4), pancreas (n = 2), bone (n = 3)	Cartilage (n = 3), fat (n = 2), striated muscle (n = 1), pancreas (n = 1), salivary gland (n = 2), hair follicle (n = 1)
4 w high dose (n = 6)	Cartilage (n = 1), lipoblasts (n = 2), pancreas (n = 2), bone (n = 3)	Cartilage (n = 3), fat (n = 5), striated muscle (n = 3), pancreas (n = 2), salivary gland (n = 2), fundic gland (n = 3), hair follicle (n = 1)	Cartilage (n = 5), lipoblasts (n = 3), pancreas (n = 3), bone (n = 1)	Fat (n = 4), striated muscle (n = 2), pancreas (n = 2), salivary gland (n = 2), fundic gland (n = 1), hair follicle (n = 1)
8 w non-treated (n = 2)			Cartilage (n = 1), pancreas (n = 1)	
8 w low dose (n = 2)	Cartilage (n = 1), pancreas (n = 1)	Striated muscle (n = 1)	Cartilage (n = 1), pancreas (n = 1), bone (n = 1)	Fat (n = 1), cartilage (n = 2), salivary gland (n = 1)
8 w high dose (n = 2)	Cartilage (n = 2), pancreas (n = 2)	Fat (n = 2), pancreas (n = 2), salivary gland (n = 1), fundic gland (n = 2)	Cartilage (n = 1), lipoblasts (n = 1), bone (n = 1)	Fat (n = 2), cartilage (n = 1), salivary gland (n = 2), fundic gland (n = 2)

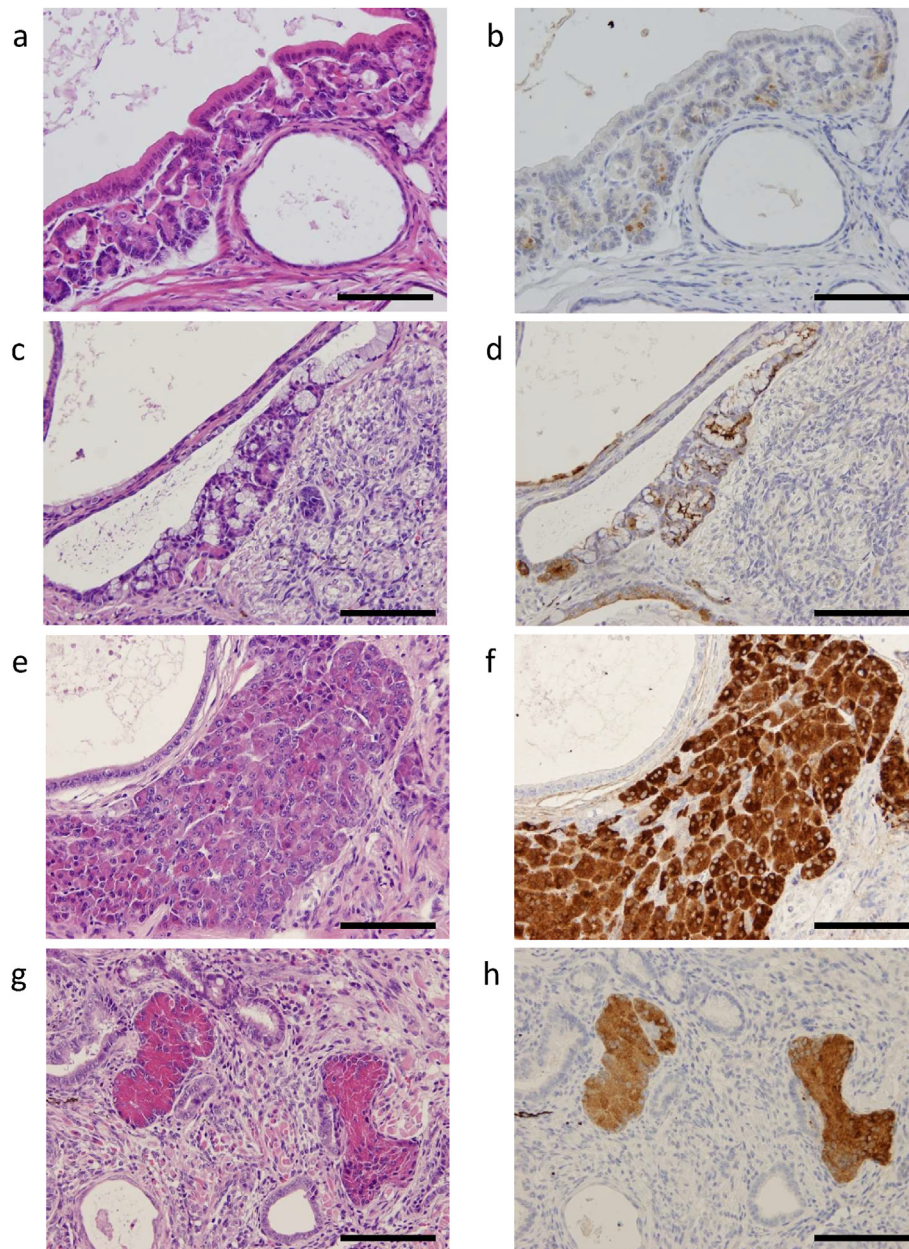


Fig. 5. Photomicrographs of immunostained and HE stained serial sections. (a, b) Fundic glands and ATP4B immunostaining. (c, d) Mature salivary glands and aquaporin 5 immunostaining. (e, f) Mature pancreas and carboxypeptidase A2 immunostaining. (g, h) Immature pancreas and carboxypeptidase A2 immunostaining. ($\times 200$, scale bar: $100 \mu\text{m}$).

any morphological changes in cisplatin-treated ESCs/iPSCs; an earlier study on embryonal carcinoma cell lines likewise found no cisplatin-induced morphological changes [11].

Our analysis of immunodeficient mice bearing ESC/iPSC-derived tumors showed that *in vivo* cisplatin treatment caused a decrease in tumor volume compared with control mice that received saline. The high dose cisplatin treatment also caused a significant decrease in the tumor necrosis score, while the maturation score showed a dose related increase compared with controls. These results are consistent with those reported for cisplatin treatment of tumors derived from an embryonal carcinoma cell line that caused inhibition of tumor growth along with differentiation of the tumor [18].

An important question is whether the increase in maturation score of teratomas in mice treated with cisplatin was due to the

elimination of immature elements or to induction of maturation by cisplatin. Our correlation analyses indicated that the necrosis score was inversely correlated with the maturation score. One possible explanation for these results is that blood supply could not keep up with the rapid increase in tumor volume, resulting in necrosis in control group. Therefore, the higher proportion of mature tissues with decreased volume after cisplatin treatment was associated with the elimination of immature elements, but was unlikely to have been due to necrosis of immature elements. Rather, we suggest that apoptosis of the immature elements occurred in teratomas of cisplatin-treated mice. The significant reduction in the frequency of proliferating cells, as shown by the PCNA-labelling index and the significantly higher ssDNA-labelling index (a marker for apoptosis in tumors [19]) is in line with this interpretation. Indeed, cisplatin has been reported to induce apoptosis in

embryonal carcinoma cells [16,18,20]. Mouse ESCs have also been reported to be hypersensitive to DNA damage and easily become apoptotic after cisplatin addition [21].

With regard to the question of whether cisplatin induced maturation, our immunohistochemical analysis demonstrated that h-Caldesmon⁺ mature smooth muscle cells were present in most specimens of mice in the 4-week high dose cisplatin group but not in untreated controls. h-Caldesmon is a good marker for mature smooth muscle cells that are often indistinguishable from fibrous tissue [22]. We also found that h-Caldesmon⁺ vascular wall emerged in specimens from all four mice in the 8-week high dose cisplatin group but not in any of the untreated controls. These results imply that maturation of teratoma tissue only occurred after cisplatin treatment. Our previous study on human immature teratomas of the ovary showed that numbers of h-Caldesmon⁺ vascular smooth muscle cells increase and Ki-67⁺ neural components decrease as the teratomas mature and the severity grade is lowered [23]. In the present study, PCNA was used as a substitute for the Ki-67 antibody that does not react with murine tissue.

It is noteworthy that mature tissues, such as mature adipose tissue, cartilage with lacunae, mature salivary glands accompanied by mucinous glands, gastric mucosa with fundic glands, mature pancreas, and hair follicles, were found in mice that had received cisplatin treatment; the absence of these mature tissues in controls indicates that they were induced by the cisplatin treatment. These mature tissues were not described in a previous histological study of mouse ESC-derived teratomas [24]. The fundic glands, mature salivary glands, and mature pancreas found here were immunopositive for ATP4B, aquaporin 5, and carboxypeptidase A2, respectively; the reliability of these antibodies has been previously demonstrated for the murine stomach [25], salivary glands [26], and pancreas [27]. The positive immunostaining identified here was not present in tissues from controls, except for immature pancreas that was immunostained by carboxypeptidase A2. Therefore, the three antibodies used here, as well as that for h-Caldesmon, may serve as good markers of differentiation when assessing murine teratomas.

In humans, CR (mature teratomatous metastasis) was first reported in immature ovarian teratomas [8]; this phenomenon also occurs in disseminated or metastatic foci of malignant mixed germ cell tumors of the ovary and testis [28,29]. CR has also been termed “transformation”, “evolution”, or “growing teratoma syndrome” [28,30]. Three possible mechanisms have been proposed for CR: first, chemotherapy induces evolution of malignant cells into benign-appearing mature tissue; second, chemotherapy selectively kills malignant cells and only benign cells remain; third, maturation occurs spontaneously rather than as a result of chemotherapy [28]. The results of the present study do not support the third possibility as mature elements only emerged in tumors after cisplatin treatment. The second suggested mechanism is consistent with our observation of slow growth rates and increased maturation score of tumors only after cisplatin treatment, presumably due to apoptosis of immature elements. However, the first mechanism may also be relevant as we found that differentiated tissues only appeared after cisplatin treatment of the tumors.

Further work is needed to provide a clearer insight into the mechanisms whereby immature teratomas are induced to differentiate by cisplatin. Since cell proliferation and differentiation show an inverse relationship [31], cell cycle withdrawal after chemotherapy may be responsible for differentiation of immature teratoma tissues. Indeed, it has been reported that cisplatin treatment of a mouse embryonal carcinoma cell line resulted in reduced expression of NANOG and POU5F1, markers of undifferentiated tissues, and increased expression of differentiation markers, similar to the effect of the differentiating agent retinoic acid [20]. In an

in vivo murine embryonal carcinoma model, combination chemotherapy that included cisplatin selectively eliminated the pluripotency factor OCT4-positive cancer stem cells [16].

This study has three main limitations: first, it is a descriptive study and does not fully explore the molecular biological basis of the phenomenon observed; second, the study was conducted using only cisplatin, and the effects of other anticancer agents such as alkaloids and topoisomerase inhibitors were not investigated; third, it is unclear whether the phenomenon that occurred is reversible as we did not investigate whether the tumors changed after discontinuation of cisplatin.

The principal finding of this study was the first identification of the generation of novel mature tissues in teratomas derived from pluripotent stem cells. This finding opens the possibility of separating these mature elements for use in transplantation. However, there are several challenges: first, since these differentiated tissues are randomly scattered through the teratoma, there is a need to develop methods for generating sufficient target tissues for separation. Longer-term dosing or a cocktail with other anticancer drugs may solve this problem. Second, it will be necessary to involve pathologists or to train researchers to confirm the histology of the target tissues. Third, even if the desired resectable tissues are obtained, it will be necessary to ensure that they can be appropriately engrafted into recipients without secondary tumorigenesis.

5. Conclusion

We demonstrated a change in ESC/iPSC-derived teratomas after treating tumor-bearing immunodeficient mice with intraperitoneal injections of cisplatin for the first time. Cisplatin treatment not only reduced the immature components of ESC/iPSC-derived teratomas but also induced them to differentiate, which was verified by immunostaining for specific markers. This property of cisplatin explains why human immature teratomas often transform into fully differentiated mature teratomas after administration of anticancer agents. The use of anticancer agents may contribute to regenerative medicine through their ability to induce differentiation of ESC/iPSC-derived teratomas.

Author contributions

A. K. contributed to conception and design of study. A. K. and M. T. performed cell and animal experiments. S.O. performed cell proliferation assay and statistical analyses. K. F. carried out immunohistochemistry. A. K. and M. K. interpreted the results. A.K. wrote the manuscript and all authors reviewed the final version.

Declaration of competing interest

The authors declare no conflicts of interests in relation to this article.

Acknowledgments

This research was supported by Grants-in-Aid for scientific research (C) [grant number 16K08675]. We thank Katsuyoshi Kumagai for conducting a pilot study, Katsuko Sudo for technical assistance, Yuichirou Harada for technical advice, and Kohsuke Kanekura for improving the manuscript.

References

- [1] Kwon SG, Kwon YW, Lee TW, Park GT, Kim JH. Recent advances in stem cell therapeutics and tissue engineering strategies. *Biomater Res* 2018;22:36.

- [2] Kumar D, Anand T, Kues WA. Clinical potential of human-induced pluripotent stem cells : perspectives of induced pluripotent stem cells. *Cell Biol Toxicol* 2017;33:99–112.
- [3] Ben-David U, Benvenisty N. The tumorigenicity of human embryonic and induced pluripotent stem cells. *Nat Rev Canc* 2011;11:268–77.
- [4] Suzuki N, Yamazaki S, Yamaguchi T, Okabe M, Masaki H, Takaki S, et al. Generation of engraftable hematopoietic stem cells from induced pluripotent stem cells by way of teratoma formation. *Mol Ther* 2013;21:1424–31.
- [5] Chan SS, Arpke RW, Filareto A, Xie N, Pappas MP, Penaloza JS, et al. Skeletal muscle stem cells from PSC-derived teratomas have functional regenerative capacity. *Cell Stem Cell* 2018;23:74–85.
- [6] Gallion H, van Nagell Jr JR, Donaldson ES, Hanson MB, Powell DF. Immature teratoma of the ovary. *Am J Obstet Gynecol* 1983;146:361–5.
- [7] Lu KH, Gershenson DM. Update on the management of ovarian germ cell tumors. *J Reprod Med* 2005;50:417–25.
- [8] DiSaia PJ, Saltz A, Kagan AR, Morrow CP. Chemotherapeutic retroconversion of immature teratoma of the ovary. *Obstet Gynecol* 1977;49:346–50.
- [9] Caldas C, Sitzmann J, Trimble CL, McGuire 3rd WP. Synchronous mature teratomas of the ovary and liver: a case presenting 11 years following chemotherapy for immature teratoma. *Gynecol Oncol* 1992;47:385–90.
- [10] Amsalem H, Nadjari M, Prus D, Hiller N, Benshushan A. Growing teratoma syndrome vs chemotherapeutic retroconversion: case report and review of the literature. *Gynecol Oncol* 2004;92:357–60.
- [11] Oosterhuis JW, Andrews PW, Knowles BB, Damjanov I. Effects of cis-platinum on embryonal carcinoma cell lines in vitro. *Int J Canc* 1984;34:133–9.
- [12] Kurata A, Hirano K, Nagane M, Fujioka Y. Immature teratoma of the ovary with distant metastases: favorable prognosis and insights into chemotherapeutic retroconversion. *Int J Gynecol Pathol* 2010;29:438–44.
- [13] Fujihara Y, Kaseda K, Inoue N, Ikawa M, Okabe M. Production of mouse pups from germline transmission-failed knockout chimeras. *Transgenic Res* 2013;22:195–200.
- [14] Lu HE, Tsai MS, Yang YC, Yuan CC, Wang TH, Lin XZ, et al. Selection of alkaline phosphatase-positive induced pluripotent stem cells from human amniotic fluid-derived cells by feeder-free system. *Exp Cell Res* 2011;317:1895–903.
- [15] Shibahara K, Uchiyama T, Fukuda T, Kura S, Tominaga Y, Maehara Y, et al. Targeted disruption of one allele of the Y-box binding protein-1 (YB-1) gene in mouse embryonic stem cells and increased sensitivity to cisplatin and mitomycin C. *Canc Sci* 2004;95:348–53.
- [16] Pierpont TM, Lyndaker AM, Anderson CM, Jin Q, Moore ES, Roden JL, et al. Chemotherapy-induced depletion of OCT4-positive cancer stem cells in a mouse model of malignant testicular cancer. *Cell Rep* 2017;21:1896–909.
- [17] Pines A, Kelstrup CD, Vrouwe MG, Puigvert JC, Typas D, Misovic B, et al. Global phosphoproteome profiling reveals unanticipated networks responsive to cisplatin treatment of embryonic stem cells. *Mol Cell Biol* 2011;31:4964–77.
- [18] Mizutani Y, Sato N, Kawauchi A, Nonomura N, Fukushima M, Miki T. Cisplatin-induced in vivo differentiation of human embryonal carcinoma. *BJU Int* 2002;89:454–8.
- [19] Watanabe I, Toyoda M, Okuda J, Tenjo T, Tanaka K, Yamamoto T, et al. Detection of apoptotic cells in human colorectal cancer by two different in situ methods: antibody against single-stranded DNA and terminal deoxynucleotidyl transferase-mediated dUTP-biotin nick end-labeling (TUNEL) methods. *Jpn J Canc Res* 1999;90:188–93.
- [20] Abada PB, Howell SB. Cisplatin induces resistance by triggering differentiation of testicular embryonal carcinoma cells. *PLoS One* 2014;9:e87444.
- [21] Kruse JJ, Svensson JP, Huigsloot M, Giphart-Gassler M, Schoonen WG, Polman JE, et al. A portrait of cisplatin-induced transcriptional changes in mouse embryonic stem cells reveals a dominant p53-like response. *Mutat Res* 2007;617:58–70.
- [22] Horita A, Kurata A, Maeda D, Fukayama M, Sakamoto A. Immunohistochemical characteristics of atypical polypoid adenomyoma with special reference to h-caldesmon. *Int J Gynecol Pathol* 2011;30:64–70.
- [23] Hongo-Kohama M, Kurata A, Hashimoto H, Fujita K, Horiuchi H, Nagao T, et al. Vascular smooth muscle cell maturation stage and Ki-67 index are diagnostic biomarkers for pathologic grade of ovarian teratoma. *Int J Gynecol Pathol* 2017;36:582–92.
- [24] Wobus AM, Holzhausen H, Jäkel P, Schöneich J. Characterization of a pluripotent stem cell line derived from a mouse embryo. *Exp Cell Res* 1984;152:212–9.
- [25] Vange P, Bruland T, Doseth B, Fossmark R, Sousa MML, Beisvag V, et al. The cytoprotective protein clusterin is overexpressed in hypergastrinemic rodent models of oxyntic preneoplasia and promotes gastric cancer cell survival. *PLoS One* 2017;12:e0184514.
- [26] Wie SM, Wellberg E, Karam SD, Reyland ME. Tyrosine kinase inhibitors protect the salivary gland from radiation damage by inhibiting activation of protein kinase C- δ . *Mol Canc Therapeut* 2017;16:1989–98.
- [27] Kelly OG, Melton DA. Development of the pancreas in *Xenopus laevis*. *Dev Dyn* 2000;218:615–27.
- [28] Hong WK, Wittes RE, Hajdu ST, Cvitkovic E, Whitmore WF, Golbey RB. The evolution of mature teratoma from malignant testicular tumors. *Cancer* 1977;40:2987–92.
- [29] Van Nguyen JM, Bouchard-Fortier G, Ferguson SE, Covens A. How common is the growing teratoma syndrome in patients with ovarian immature teratoma? *Int J Gynecol Canc* 2016;26:1201–6.
- [30] Logothetis CJ, Samuels ML, Trindade A, Johnson DE. The growing teratoma syndrome. *Cancer* 1982;50:1629–35.
- [31] Ruijtenberg S, van den Heuvel S. Coordinating cell proliferation and differentiation: antagonism between cell cycle regulators and cell type-specific gene expression. *Cell Cycle* 2016;15:196–212.